7. SITE 915[1]

Shipboard Scientific Party[2]

HOLE 915A

Date occupied: 5 October 1993

Date departed: 7 October 1993

Time on hole: 2 days, 12 hr

Position: 63°28.285′N, 39°46.909′W

Bottom felt (drill-pipe measurement from rig floor, m): 544.0

Distance between rig floor and sea level (m): 10.89

Water depth (drill-pipe measurement from sea level, m): 533.1

Total depth (from rig floor, m): 752.7

Penetration(m): 209.4

Number of cores (including cores with no recovery): 26

Total length of cored section (m): 209.4

Total core recovered (m): 32.84

Core recovery (%): 15.7

Oldest sediment cored:
Depth (mbsf): 196.8
Nature: volcanic clay with gravel
Age: Eocene
Measured velocity (km/s): 4.0

Hard rock:
Depth sub-bottom (m): 209.4
Nature: basalt
Measured velocity (km/s): 3.9

Basement:
Depth sub-bottom (m): 209.4
Nature: basalt
Measured velocity (km/s): 3.9

Principal results: Site 915 is located on the East Greenland Shelf, approximately 58 km from the Greenland coast. After an unsuccessful attempt to reach basement at Site 914, *JOIDES Resolution* sailed to an alternative site on the shelf, about 3 km to the northwest. Seismic profiles indicate that the glacial sediment cover at Site 915 is thinner than at Site 914. The primary objectives of this site were the same as those at Site 914, namely (1) Quaternary and Holocene glacial history of the margin; (2) Paleogene sedimentation and subsidence history; and (3) the composition, age, and eruption environment of the seaward-dipping reflector sequences (SDRS).

Three lithological units were recognized in the cored section (Fig. 1). Recovery of Unit I, glaciomarine mud and sand with dropstones, was poor, but allowed division into two subunits. Subunit IA (0–2.2 mbsf) is Pleistocene to Holocene glaciomarine silty sand and silty mud with dropstones. A short length of compacted diamicton was recovered at the base of the subunit. Subunit IB (2.2–84.8 mbsf) is presumed to be a diamicton with gneiss, basalt, metasediment, and granitic pebbles and cobbles. No matrix was recovered from this subunit. We presume the age to be Quaternary.

Lithologic Unit II (84.8–187.1 mbsf) is composed of upper middle Eocene and upper Eocene volcaniclastic silty sandstone and sandy siltstone with interbeds of calcareous mudstone and sandstone. The unit was divided into three subunits. Subunit IIA (84.8–148.8 mbsf) is predominantly black and dark gray and heavily bioturbated. It comprises siltstone, minor calcareous siltstone, and mudstone. The major source for most of the sediment was volcanic, but a significant component from the Precambrian metamorphic terranes of Greenland also was observed. Plant fragments are scattered through the subunit. Subunit IIB (148.8–168.0 mbsf) is a dusky red and laminated volcaniclastic clayey silt with sand. The primary source material for this subunit was probably lateritized basalt. Subunit IIC (168.0–187.1 mbsf) is lithologically similar to Subunit IIA. Sedimentary facies and benthic foraminifers are consistent with Unit II having been deposited in shallow water at shelf or upper-slope depths.

Unit III (187.1–189.3 mbsf) comprises a heterolithic conglomerate with gravel, sand, and silt. The clasts in the conglomerate are predominantly basalt, and the unit overlies a red, weathered basalt (saprolite). This lithologic unit was probably deposited in a subaerial environment, possibly an alluvial fan.

The igneous succession (189.3–209.4 mbsf) consists of two basalt units: an upper, 1.05-m-thick, highly oxidized basalt flow, and 4 m of slightly altered, vesicular basalt. The two flows are separated by several basalt cobbles, indicating that they are not contiguous. The lower basalt contains glomerocrysts of olivine, plagioclase, and pyroxene. The composition of the basalts, especially the high Zr/Nb ratios, indicates derivation from a depleted, mid-ocean ridge basalt mantle source. Alteration is restricted to clay, zeolite, and chlorophaeite(?) linings in vesicles and about 5% clay in the groundmass.

Nannofossils confirm a Quaternary (<1.7 Ma) age for lithologic Subunit IB, an upper Eocene age for Subunit IIA, and an upper middle Eocene age for Subunit IIC. We were unable to obtain an age for Unit III. Planktonic foraminifers are consistent with these ages. Benthic foraminifers indicate a paleowater depth of less than 250 m for Subunit IIA.

Paleomagnetic data were obtained from seven cores in Hole 915A. Core 152-915A-16R carries a normal polarity magnetization. Biostratigraphic data do not permit a firm correlation to the geomagnetic time scale; the magnetozone could represent Chrons C15n or C16n-1n or C16n-2n. Cores 152-915A-18R through -22R are all reversely magnetized. Both Cores 152-915A-21R and -22R are of middle Eocene age (38–41 Ma), and correlation with Chron C18r has been tentatively proposed. The reverse polarity remanence in Cores 152-915A-18R to -20R probably records the same chron. Core 152-915A-24R through the upper part of the volcanic basement is reversely magnetized. Stratigraphic arguments, based on the age of the magnetic anomalies in this area, suggest an age of Chron C24r.

Interstitial-water samples were taken from the core in Hole 915A. A decrease in dissolved chloride is observed as basement is approached. This suggests that fresh, low-chloride water from layers within the basalt discharges into the sediments. Monitoring of hydrocarbons C_1 to C_3 showed no significant amounts of gases in the sediments at Site 915. Elevated yields of organic carbon probably result from wood fragments.

Carbonate contents are between 0% and 5%, with values up to 38% in highly cemented sandstones.

The diamictons recovered at Site 915 are strongly consolidated and have shear strengths greater than the range covered by handheld penetrometers. This suggests that these sediments have been in contact with ice sheet(s) on the East Greenland Shelf. Synthetic seismic modeling of deep

[1] Larsen, H.C., Saunders, A.D., Clift, P.D., et al., 1994. *Proc. ODP, Init. Repts.*, 152: College Station, TX (Ocean Drilling Program).
[2] Shipboard Scientific Party is as given in list of participants preceding the contents.

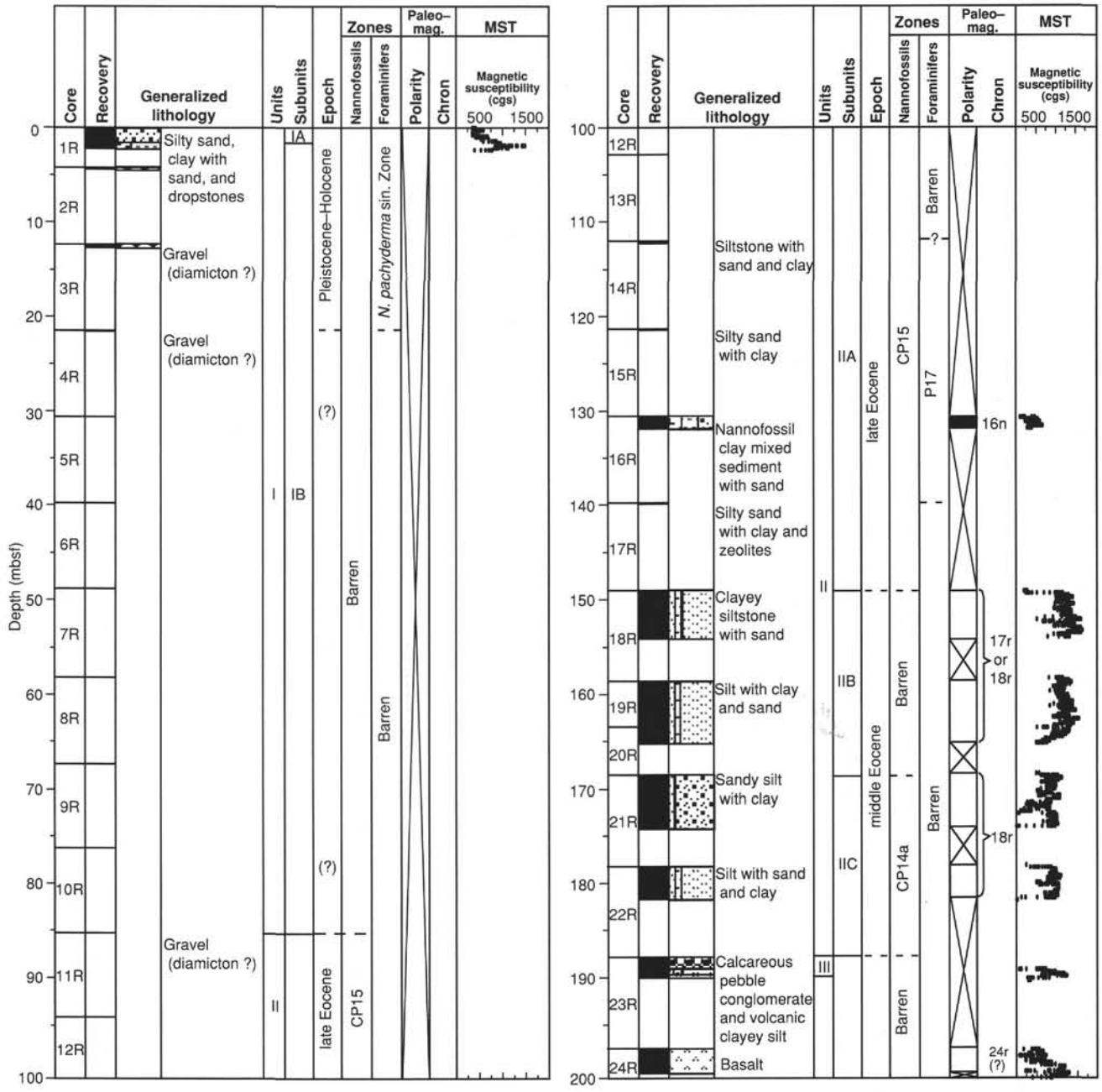

Figure 1. Site summary for Site 915.

(≈30 m above basement), interbedded volcaniclastic sands and silts enabled us to correlate in detail the core to the seismic data.

Principal Findings at Site 915 include the following:

1. Drilling at Site 915 demonstrated the presence of basaltic basement beneath sediment of upper middle Eocene age.
2. The basalt has been extensively weathered, probably in a subaerial environment, and the immediately overlying sediment (Unit III) appears to be alluvial in origin.
3. The predicted age of the basalts (lower Eocene) is considerably older than the sediments, and this will require confirmation by Ar-Ar dating of the basalt; suitable feldspar-rich basalt has been recovered.
4. The recovery of Eocene sediments will provide important data for studies of the subsidence history of the shelf.
5. The presence of diamicton confirms that wet-based glaciers advanced to at least this point on the shelf, about 55 km east of the present ice sheet.

OPERATIONS

Hole 915A

At 0030 hr on 5 October, the Site 914 beacon was turned off, and at 0130 hr the vessel was offset to the new location in dynamic positioning (DP) mode (all times are in Universal Time Coordinated, UTC, unless otherwise noted). The first beacon on Site 915 was dropped at 0215 hr. A second beacon was deployed at 0237 hr, after the first beacon was automatically released almost immediately upon hitting the mudline. The SEDCO Electrical Superintendent considered that the beacon had been released by precision depth recorder pulses, which are very strong at a depth of only 500 m.

After the vessel had stabilized on location, a rotary-core-barrel bottom-hole assembly (RCB BHA), without a bit release, was lowered. An RCB mudline core was obtained by gently lowering the drill

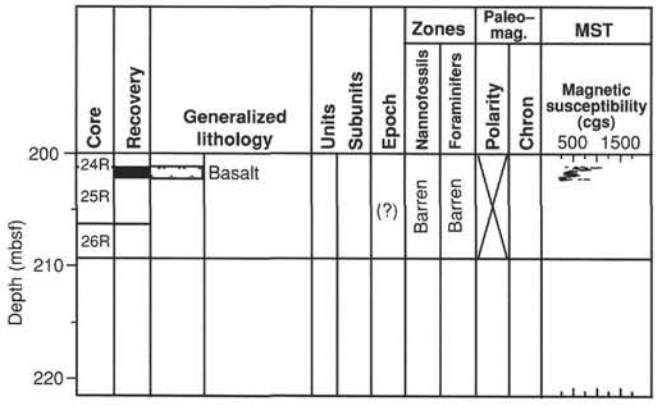

Figure 1 (continued).

string and observing the heave compensator action; weight was taken at a depth of 533.1 m. This was considered to be the depth of this site.

RCB coring commenced at 0500 hr on 5 October and advanced to 206.4 mbsf (Core 152-915A-25R). The coring history at Site 915 is summarized in Table 1. After the core barrel was withdrawn, flow-back from the pipe indicated that the flapper was jammed open, probably by a hard rock fragment. A chisel bit deplugger was dropped and recovered, and the flow-back ceased. After the core barrel was dropped for Core 152-915A-26R, the bit was lowered to the bottom of the hole, and coring resumed. Immediately, torquing of 200 to 400 A was evident. The drilling crew assumed that the rock fragment, cleared with the chisel deplugger, had dropped to the bottom of the hole. After working the drill bit for 4 hr in an attempt to grind down this material, drilling advanced only 3 m. With only 32 hr on bit, the drilling crew prepared for a bit trip. The core barrel was retrieved and contained only a 0.04-m piece of rock.

A free-falling funnel (FFF) was made up and dropped at 1155 hr on 7 October. The vibration-isolated television camera was run into the hole; it verified that the FFF was upright on the bottom of the hole. The BHA was pulled out of the hole, and the bit arrived on deck at 1415 hr. All four cones and four core guides were missing. The drilling crew inferred that what they had assumed was a rock fragment was either part of the core guides, or a cone that had dropped off after the core barrel had been landed. The large amount of metal debris in the hole thwarted plans for further coring. The beacon was turned off and left in place to facilitate a return to the site, should that be necessary. The vessel was offset in DP mode approximately 2.2 km north to Site 916 (proposed Site EG63-1B).

LITHOSTRATIGRAPHY

Introduction

Site 915 is located near the middle of a short (approximately 6 km long) transect across part of the East Greenland Margin, which includes Sites 914, 916, and 917 (see also, "Stratigraphic Summary" chapter, this volume). The sediment in Hole 915A is divided into three lithologic units that overlie weathered basalt (Table 2). Total thickness of drilled sediment is 189.3 m. A summary of the major characteristics and ages of the recovered sediment is given in Table 2. Quaternary glacial sediment (lithologic Unit I, 93.7 m thick) overlies Eocene marine silty sand and sandy silt (lithologic Unit II, 93.4 m thick). The lowest sedimentary deposit (lithologic Unit III, 2.15 m thick) is a matrix-supported polymict conglomerate with breccia and sandstone. We divided lithologic Unit I into two subunits based on degree of compaction, and lithologic Unit II into three subunits on the basis of a marked change in color and microfossil composition.

Table 1. Coring summary, Site 915.

Core	Date (Oct. 1993)	Time (UTC)	Depth (mbsf)	Length cored (m)	Length recovered (m)	Recovery (%)
152-915A-						
1R	5	0615	0.0–4.3	4.3	2.33	54.2
2R	5	0845	4.3–12.3	8.0	0.26	3.3
3R	5	1415	12.3–21.4	9.1	0.45	4.9
4R	5	1730	21.4–30.5	9.1	0.5	0.6
5R	5	2100	30.5–39.6	9.1	0.00	0.0
6R	5	2240	39.6–48.7	9.1	0.00	0.0
7R	6	0015	48.7–57.8	9.1	0.00	0.0
8R	6	0130	57.8–67.0	9.2	0.00	0.0
9R	6	0300	67.0–75.9	8.9	0.00	0.0
10R	6	0400	75.9–84.8	8.9	0.00	0.0
11R	6	0510	84.8–93.7	8.9	0.00	0.0
12R	6	0630	93.7–102.9	9.2	0.00	0.0
13R	6	0730	102.9–112.0	9.1	0.00	0.0
14R	6	0900	112.0–121.2	9.2	0.35	3.8
15R	6	1000	121.2–130.3	9.1	0.13	1.4
16R	6	1110	130.3–139.5	9.2	1.44	15.6
17R	6	1205	139.5–148.6	9.1	0.07	0.8
18R	6	1410	148.6–158.1	9.5	5.12	53.9
19R	6	1530	158.1–162.9	4.8	5.47	114.0
20R	6	1820	162.9–167.9	5.0	1.95	39.0
21R	6	2000	167.9–177.5	9.6	5.87	61.1
22R	6	2100	177.5–187.1	9.6	3.56	37.1
23R	6	2320	187.1–196.8	9.7	2.15	22.1
24R	7	0200	196.8–201.4	4.6	2.67	58.0
25R	7	0500	201.4–206.4	5.0	0.93	18.6
26R	7	1100	206.4–209.4	3.0	0.04	1.3
Coring totals:				209.4	32.84	15.7

Lithologic Units

Lithologic Unit I: Glaciomarine mud with dropstones and diamicton
Interval: Sections 152-915A-1R to -10R-CC
Depth: 0–84.8 mbsf
Thickness: 84.8 m (maximum)
Age: Quaternary

Lithologic Unit I is divided into two subunits: an upper glaciomarine subunit (lithologic Subunit IA) and a lower, more compacted subunit, a diamicton (lithologic Subunit IB). Poor recovery in lithologic Unit I, caused by the presence of glacial erratics and dropstones, limited the amount of data collected. However, it is evident that a thin deposit of glaciomarine sediment overlies more compacted diamicton.

Lithologic Subunit IA: Glaciomarine mud with dropstones
Interval: Core 152-915A-1R
Depth: 0–2.2 mbsf
Thickness: 2.2 m
Age: Quaternary

Lithologic Subunit IA is glaciomarine. Poorly sorted sandy silt, silty sand, and sandy mud with many dropstones contains marine microfossils (nannofossils, foraminifers, and diatoms). The subunit is thin and occurs only in Core 152-915A-1R. A more compact deposit was recovered over interval 152-915A-1R2, 0–70 cm, and Section 152-915A-1R-CC. Dropstones within Subunit IA mainly comprise lithologies characteristic of the southeast Greenland coast: granite, gneiss, and basalt. In smear slides and grain mounts, the nature of the source rock areas is even more apparent. Zircon, sphene, blue-green amphibole, clinopyroxene, and garnet are common. Quartz is the most abundant mineral and makes up more than 30% of smear slide components, followed in abundance by feldspar, amphibole, and rock fragments. X-ray diffractograms (intervals 152-915A-1R-1, 79–80 cm, and 135–136 cm) show the presence of quartz, plagioclase feldspar, orthoclase feldspar, amphibole, biotite, chlorite, and calcite. Many of the heavy minerals and quartz grains are well rounded.

Table 2. Summary of lithologic units at Hole 915A.

Lithologic unit	Lithology	Depth (mbsf)	Core intervals	Thickness (m)	Age
		0–84.8	152-915A-1R-1, 0 cm, to -11R-CC	84.8	
IA	Silty sand with dropstones; glaciomarine	0–2.2	152-915A-1R-1, 0 cm, to -1R-CC	2.2	Quaternary
IB	Diamicton with cobble and pebble clasts	2.2–84.8	152-915A-2R through -10R	82.6	Quaternary
		84.8–187.1	152-915A-11R through -22R-CC	102.3	
IIA	Black and dark gray sandy silt and silt with clay; minor calcareous mudstone and sandstone	84.8–148.8	152-915A-11R to -18R-1, 20 cm	64.0	latest Eocene
IIB	Dusky red clayey silt and silt with sand	148.8–168.8	152-915A-18R-1, 20 cm, to -21R-1, 7 cm	19.2	late Eocene
IIC	Black and dark gray sandy silt and silt with clay; minor calcareous mudstone and sandstone	168.0–187.1	152-915A-21R-1, 7 cm, through -22R-CC	19.1	late middle Eocene
III	Red and black conglomerate and breccia, sandstone, and siltstone; overlies weathered basalt	187.1–189.3	152-915A-23R-1, 0 cm, to -23R-2, 70 cm	2.2	??

Lithologic Subunit IB: Diamicton
Interval: Sections 152-915A-2R-1 to -11R-CC
Depth: 2.2–84.8 mbsf
Thickness: 82.6 m (maximum)
Age: Quaternary

Lithologic Subunit IB is probably a glacial diamicton. However, because only a few clasts were recovered, we base that interpretation on studies of seismic profiles over and near the site, on the compositions and sizes of the recovered clasts, on correlation with similar sediments at Sites 914 and 916, and on operational difficulties that were associated with drilling and coring of this cobble-rich sequence. The clasts are predominantly gneiss, granite, metabasalt, and metagabbro. No fossils were recovered from this subunit.

Lithologic Unit II: Mixed volcaniclastic and siliciclastic silty sand and sandy silt with variable amounts of clay, interbeds of calcareous mudstone and calcareous sandstone.
Interval: Sections 152-915A-11R-1 to -22R-CC
Depth: 84.8–187.1 mbsf
Thickness: 102.3 m
Age: late middle Eocene and late Eocene

Lithologic Unit II is predominantly a sequence of mixed volcaniclastic and siliciclastic silty sand and sandy silt, with variable amounts of clay. Calcareous mudstone, calcareous sandstone, silty clay, and clayey silt are also present. Lithologic Subunits IIA and IIC are similar in color (black and dark gray), lithology (bioturbated silty sand and sandy silt, with interbeds of calcareous mudstone and calcareous sandstone), and composition (mostly volcaniclastic). In contrast, lithologic Subunit IIB is dusky red and laminated, although it is also predominantly volcaniclastic. Subunit IIB has no calcareous mudstone or calcareous sandstone beds.

Lithologic Subunit IIA: Black and dark gray silty sand and sandy silt, with variable amounts of clay, and interbeds of olive black and dark olive gray calcareous mudstone and calcareous sandstone
Interval: 152-915A-11R-1, 0 cm, to -18R-1, 20 cm
Depth: 84.8–149.8 mbsf
Thickness: 64.0 m
Age: late Eocene

Nannofossils from this subunit are latest Eocene (CP14) in age. There was no recovery in Cores 152-915A-12R and -13R. However, we think that the upper Eocene sequence was drilled, beginning with Core 152-915A-11R, because a very small amount (a few grams) of sediment from along the plastic liner of Core 152-915A-11R yielded uppermost Eocene nannofossils. The first coherent sediment recovered from this subunit was calcareous sandstone in the interval 152-915A-14-1, 0–35 cm (112.0–112.35 mbsf).

Lithologic Subunit IIA is predominantly black and dark gray and is heavily bioturbated (Fig. 2). These black and dark gray beds are dominantly sandy silt with clay and silty sand with clay. Most primary sedimentary structures were destroyed by extensive bioturbation. In places, faint bedding can be discerned. Olive black and dark gray calcareous sandstone and calcareous mudstone beds, as thick as 20 cm, stand out in stark contrast to the more abundant black silty sands and sandy silts. A heavily bioturbated calcareous mudstone bed (Fig. 3) in the interval 152-915A-16R-1, 111–118 cm, has sand, silt, and clay mixed in a micrite matrix. An excellent example of a calcareous sandstone and calcareous mudstone interbed is in interval 152-915A-18R-1, 0–20 cm, where it forms the base of Subunit IIA (see core photo). (See photograph in "Cores" Section, this volume.)

The composition of lithologic Subunit IIA shows that the major source terrain for most of the sediment was volcanic, but a contribution from the Precambrian igneous and metamorphic rocks of the Greenland craton was also significant. Our interpretation of volcanic provenance is supported by the abundance of deeply weathered basaltic rock fragments, opaque minerals, rounded clinopyroxene, and the rare presence of clay-rich rock fragments that still have primary shard-like outlines, which suggests that these are altered volcanic glass and glassy rock fragments. In addition, phillipsite is abundant (up to 10% in some smear slides). Phillipsite is common in diagenetically altered volcanic sediment, particularly in basaltic material (Kastner, 1979). Sediment contributions from Precambrian rocks are suggested by a relatively large amount (10%–20%) of quartz, the ubiquitous presence of blue-green amphibole, some well-rounded garnet grains, and the occurrence of muscovite and biotite. Large and well-rounded quartz grains are ubiquitous and make up as much as 10% of some smear slides. These quartz grains, about 3 mm in diameter, are partly coated with limonite, and many are indented with relatively fresh percussion marks. The characteristics of the quartz grains imply (1) long transport (or several episodes of transport); (2) a high energy medium, at least during the last transport episode; and (3) a phase of limonite cementation. We presume that their presence implies uplift and deep erosion of the eastern Greenland craton during the late Eocene. Streams having high gradients or passage through a neritic environment may have been responsible for the rounding and percussion marks. Plant fragments are scattered throughout lithologic Subunit IIA. Most are small and partly decomposed, but their presence signifies a warmer and more humid climate during the late Eocene than at present.

Lithologic Subunit IIB: Dusky red and laminated volcaniclastic clayey silt with sand and silty clay with sand
Interval: 152-915A-18R-1, 20 cm, to -21R-1, 7 cm
Depth: 148.8–168.0 mbsf
Thickness: 19.2 m
Age: No fossils seen; probably late Eocene

Lithologic Subunit IIB is dusky red and laminated, and thus distinctive from the black and dark gray subunits above and below, which are similar to each other in both composition and color. Dark reddish brown, thin (less than 2 cm) laminae are separated by thicker (2–10 cm), dusky red beds. Small perturbations along the lower bedding planes of some thin laminae may be cut-and-fill structures.

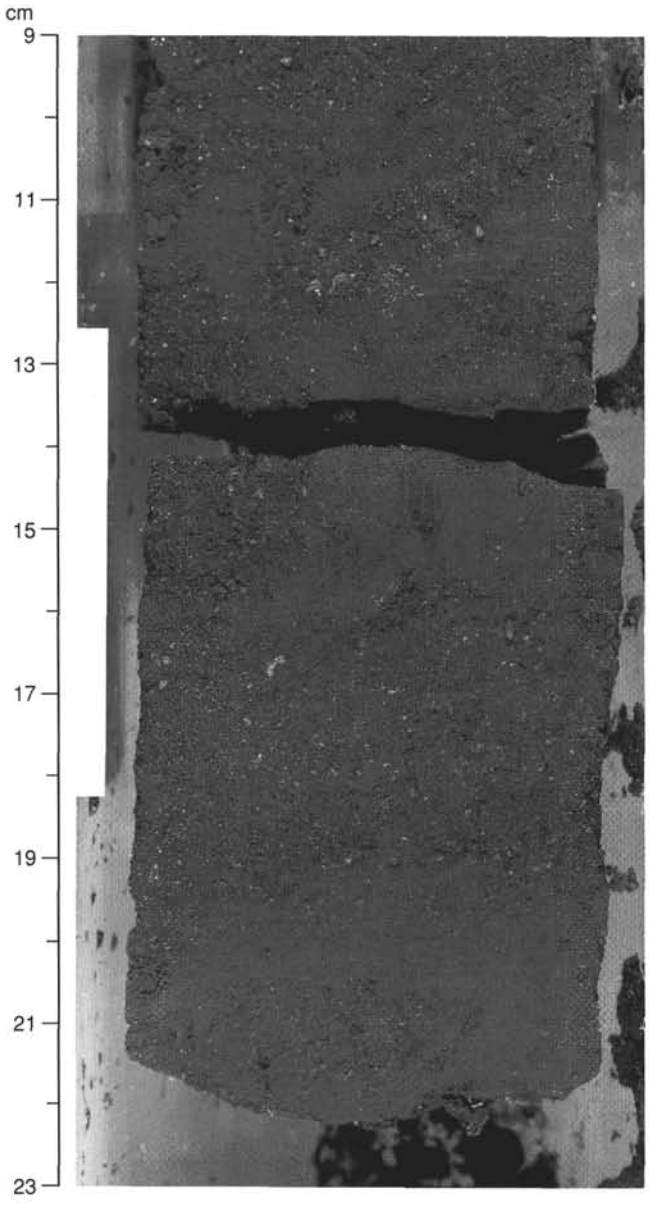

Figure 2. Black, heavily bioturbated sandy silt with clay, lithologic Subunit IIA (interval 152-915A-16R-1, 9–23 cm).

Pyrite-filled burrows are more common in the upper part of the subunit and become rarer with depth. Laminae dip as much as 5° consistently in one direction.

The sediment is mostly clayey silt with sand and silty clay with sand. The thin laminae are made up of sandy silt with clay. Major components are strongly weathered volcanic rock fragments (including some probable altered glass), red, semi-opaque particles (Fe-oxides and Fe-hydroxides of undetermined composition that make up 40% of one smear slide), clay, opaque minerals (5%–15%), and quartz (generally less than 10%). None of the large quartz grains, described in lithologic Subunit IIA above, were found in smear slides from this subunit. Epidote, amphibole, and phillipsite (partly dissolved), are minor constituents. Clinopyroxene grains occur in trace amounts; some smear slides have none at all. X-ray diffractograms show the presence of kaolinite, illite, smectite, and quartz in the Sample 152-915A-18R-1, 54–55 cm, and in addition, a high-Mg calcite in sediments from Sample 152-915A-18R-3, 28–29 cm, in a coarse-grained lamination.

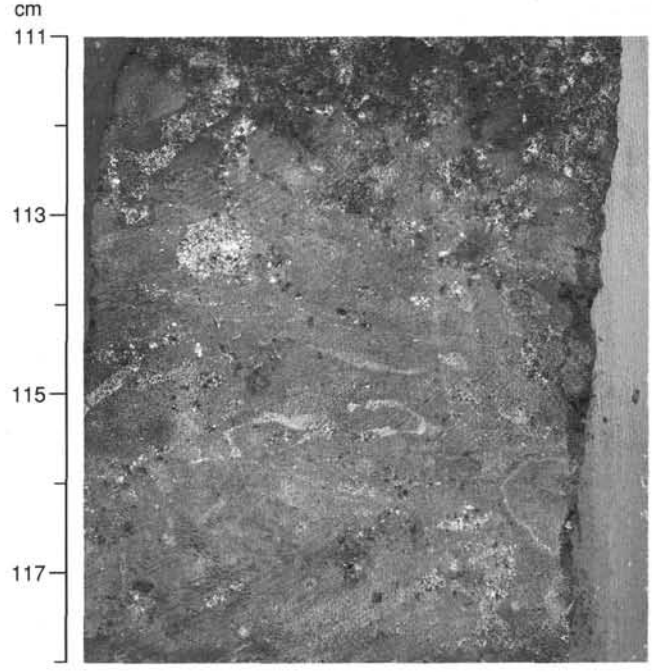

Figure 3. Calcareous mudstone interbedded with black silt and sand, lithologic Subunit IIA (interval 152-915A-16R-1, 111–118 cm). Similar sediment comprises Subunit IIC.

Characteristics of Subunit IIB imply that the source area mainly was made up of basaltic rocks having a thick lateritic soil cover. Chemical weathering concentrated kaolinite and Fe-oxide components and destroyed most primary minerals in the basalt.

The age of Subunit IIB is unknown, but it is bounded stratigraphically by sediments below and above of late middle Eocene and latest Eocene age, respectively. It is most likely late Eocene in age.

Lithologic Subunit IIC: Black and dark gray sandy silt and silty sand, with variable amounts of clay, and interbeds of olive black and dark olive gray calcareous mudstone and calcareous sandstone
Interval: 152-915A-21R-1, 7 cm, to Section 152-915A-22R-CC
Depth: 168.0–187.1 mbsf
Thickness: 19.1 m
Age: late to middle Eocene

Lithologic Subunit IIC is similar to lithologic Subunit IIA. The sediments are highly bioturbated, and bedding is difficult to recognize. Olive black and dark gray calcareous sandstone and calcareous mudstone beds, as much as 20 cm thick, stand out from the black silts and sands that make up the bulk of lithologic Subunit IIC.

The silt and sand are mostly of volcaniclastic origin. Smear slides and grain mounts show large percentages of altered volcanic rock fragments, altered volcanic glass and opaque minerals, plus smaller amounts of clinopyroxene (trace to 3%), phillipsite (1%–5%), amphibole (trace to 3%), and chlorite (trace to 2%). Quartz grains make up 10% to 15%, and feldspar comprises 3% to 10%. Large quartz grains with limonite stains (such as those described from lithologic Subunit IIA) are rare in Subunit IIC. An X-ray diffractogram from Sample 152-915A-21R-1, 85–87 cm, shows the presence of quartz, plagioclase, smectite, and kaolinite. Plant fragments are common. Nannofossils provide a late middle Eocene age.

Calcareous sandstone and mudstone beds are similar to those found in Subunit IIA. One thin section of calcareous sandstone was point-counted (500 points) and found to have the following composition: quartz, 19%; glauconite, 24%; sparry calcite cement, 41%; amphibole, 3%; rock fragments (granitic and volcanic), 3%; feldspar,

3%; opaque minerals, 4%; and epidote, glass, and mica, all 1% each. The glauconite grains are both fresh green and oxidized red.

All subunits of lithologic Unit II were deposited in shallow water at shelf and upper-slope depths, according to studies of benthic foraminifers (see "Biostratigraphy" section, this chapter). The dusky red sediment of this unit can be considered as one facies association, with Subunits IIA and IIC representing more distal, outer-shelf deposits and Subunit IIB representing possibly a more proximal, pro-delta deposit.

Lithologic Unit III: Conglomerate, breccia, gravels, sands, and silts
Interval: 152-915A-23R-1, 0 cm, to -23R-2, 70 cm
Depth: 187.1–189.3 mbsf
Thickness: 2.2 m
Age: Unknown

Lithologic Unit III overlies basalt. A conglomerate, which dominates lithologic Unit III in the upper part, is poorly sorted and has well-rounded to angular clasts that have been set in a red sand and silt matrix. The conglomerate is interbedded with sandstone (Fig. 4). Clasts in the conglomerate and associated unconsolidated gravel are predominantly basaltic, with uncommon to rare clasts of dolerite, quartzite(?), claystone, sandstone, and gabbro. The clastic rocks grade downward into a crudely bedded red basalt breccia, with a red sand and silt matrix and overlying weathered basalt. The red color and character of lithologic Unit III suggest that this sediment was deposited in a subaerial environment, possibly in an alluvial fan. The top of the breccia is weathered, with characteristics of the base of a soil (see "Shelf Summary" chapter, this volume).

BIOSTRATIGRAPHY

Calcareous Nannofossils

Sample 152-915A-1R-CC is barren of calcareous nannofossils. Going downhole, the next sedimentary sample suitable for nannofossil analysis is from Sample 152-915A-11R-CC. The interval from this sample through Sample 152-915A-17R-CC yielded common nannofossils of late Eocene age, including several age-diagnostic species such as *Reticulofenestra reticulata, R. umbilicus*, and *Isthmolithus recurvus*. Samples 152-915A-18R-CC through -20R-CC are barren of nannofossils. Several samples from different lithologies in Core 152-915A-21R were examined for nannofossils. Sample 152-915A-21R-1, 2 cm (from the "red clay") is barren of nannofossils, while Sample 152-915A-21R-1, 4 cm (from a black volcanic sand sequence, the major lithology of the core) is fossiliferous, with *Chiasmolithus solitus, Reticulofenestra umbilicus, Isthmolithus recurvus*, among other middle Eocene species identified. Sample 152-915A-21R-3, 3 cm (a calcitic sand interval), is barren of nannofossils. Sample 152-915A-21R-CC contains an assemblage of middle Eocene age (Zone CP14a). Sample 152-915A-22R-CC yielded rare specimens of *Chiasmolithus solitus* and *Reticulofenestra umbilicus*, among a few other species, and has been assigned to Zone CP14a (Fig. 5). Sample 152-915A-23R-2, 6 cm (a soft-sediment layer directly above the weathered basalt), is barren of nannofossils.

Planktonic Foraminifers

At Site 915, planktonic foraminifers were analyzed in the core catchers, as well as a few additional samples. Sample 152-915A-1R, 0–2 cm, contains moderately preserved, common planktonic faunas consisting of sinistrally coiled specimens of *N. pachyderma, G. bulloides, Globigerinita glutinata,* and *Globigerinita juvenilis*, along with rarer specimens of *Neogloboquadrina dutertrei* and *Globorotalia inflata*, and abundant sponge spicules and gastropod fragments. This assemblage can be attributed to the upper part of *N. pachyderma* sinistral coiling Zone (Pleistocene–Holocene), whereas that from Sample 152-915A-IR-CC, containing only a few sinistrally coiled specimens of *N. pachyderma*, may be attributed to the middle to lower part of the same zone.

Planktonic foraminifers are absent in the glaciomarine sediment below Core 152-915A-1R. They occur only infrequently in the Paleogene sediment below the glacial tills.

Sample 152-915A-15R-CC contains rare specimens of *Chiloguembelina* sp. and a single specimen of *Globoquadrina tapuriensis*. These two species are indicative of late Eocene–Oligocene age. As the first occurrence of *G. puriensis* is documented from the uppermost Eocene (Coccioni et al., 1988; Premoli Silva and Spezzaferri, 1990) comparison with the nannofossil record allows attribution of, this assemblage to the upper part of Zone P17 of Berggren and Miller (1988) in the uppermost Eocene.

Samples 152-915A-16R-CC and -17R-CC contain very rare and poorly preserved specimens of the long-range species *"Globigerina" venezuelana, Globorotaloides suteri*, and *Globorotaloides variabilis*. These species are not age-diagnostic, but nannofossil assemblages suggest a late Eocene age for this interval (Fig. 5). Samples 152-915A-18R-CC through to 22R-CC are barren of planktonic foraminifers.

Benthic Foraminifers

Benthic foraminifers were identified in Sample 152-915A-1R, 0–2 cm, and in Samples 152-915A-1R-CC and -14R-CC to -22R-CC.

Within the recovered Quaternary succession, the preservation of benthic formininifers is moderate. Benthic foraminifers contribute 50% and 30% of the total foraminiferal fauna in Samples 152-915A-1R, 0–2 cm, and -1R-CC, respectively. The assemblage of Sample 152-915A-1R, 0–2 cm, consists mainly of *Cibicides lobatulus, Cibicides refulgens*, and *Cibicides* spp. This assemblage probably represents a post-glacial, Holocene environment because this sample was taken from just below the modern seafloor. In Sample 152-915A-1R-CC, *Cassidulina norvangi, Cassidulina teretis, Cibicides refulgens*, and *Elphidium excavatum* are common. *Cassidulina teretis* is a dominant species during Pliocene to Pleistocene glacial intervals of the North Atlantic region (Murray, 1984).

Within the recovered Paleogene sediment (Samples 152-915A-14R-CC to 22R-CC), benthic forms constitute virtually 100% of the foraminiferal fauna. One exception is Section 152-915A-14R-CC, which is barren of benthic foraminifers. Nevertheless, benthic faunas are very rare, and preservation is poor in these sections. Sample 152-915A-19R-CC is distinctive in showing a moderate preservation. The assemblages found within Samples 152-915A-15RCC to -17R-CC are characterized by the occurrence of *Cibicidoides* spp. In Sample 152-915A-15R-CC, in addition to the above mentioned genus, *Buliminclia* sp. and *Lenticulina* sp. occur. The combination of *Cibicidoides* sp. and *Lenticulina* sp. was reported from some Eocene samples at DSDP Sites 403 and 404 on the Rockall Plateau, in the North Atlantic. The paleowater depth inferred from the assemblages in these samples varied from normal marine, inner shelf (shallower than 75 m), to epibathyal (shallower than 600 m; Murray, 1979). Therefore, the assemblage in Sample 152-915A-15R-CC may suggest a normal marine environment and a paleowater depth of 0 to 600 m. Samples 152-915A-18R-CC to -20R-CC are characterized by the occurrence of *Uvigerina abbreviata* and/or *Uvigerina* sp. Samples 152-915A-21R-CC and -22R-CC contain *Stilostomella* sp. However, abundances of benthic foraminifers in these sections are too low to discuss paleoenvironment, except for their being deposited in water shallower than the calcium carbonate compensation depth (CCD) (Fig. 5).

PALEOMAGNETISM

Paleomagnetic data were obtained from seven cores in Hole 915A. Cores 152-915A-16R, and -18R through -22R are volcanogenic Eocene sandstones and siltstones. From Core 152-915A-24R, coherent in-situ pieces of volcanic rocks were recovered that form the basement at this site. The magnetostratigraphy of Hole 915A is summarized in Figure 6.

Most of the remanence data from Hole 915A are from WCC studies of the archive-half sections. This information has been sup-

plemented by data from three discrete specimens that were measured using the MSM and AF demagnetized to 80 mT. Initial natural remanent magnetization intensities of the sedimentary rocks generally range from 100 to 300 mA/m.

Demagnetization to 30 mT reduced the intensities to typically 30% to 10% of the initial value. In most cases, the sedimentary rocks carry two main components of magnetization. A low-coercivity component (probably drilling induced) is generally isolated by the 10-mT demagnetization. The characteristic primary direction is usually defined after the 20- or 30-mT demagnetization step. Demagnetization of two discrete samples from Core 152-915A-19R reveals a high-coercivity component that is not cleaned after the 80-mT AF treatment (Fig. 7). Considering the presence of pyrite-filled burrows in this core, this high-coercivity component is possibly carried by a ferromagnetic sulfide. In addition to the standard remanence investigations (Fig. 8), isothermal remanent magnetization (IRM) analyses were performed on one specimen from the lava sequence (152-915A-24R-2, 52 cm) to determine its remanence carrier(s). The specimen saturated at 0.3T and had a peak IRM value of 378 A/m. This information suggests that the remanence of this specimen probably was carried by titanomagnetite.

Core 152-915A-16R (130.3–131.6 mbsf) carries a normal polarity magnetization having a characteristic mean inclination of 60° to 70° (Fig. 6). Nannoplankton data (see "Biostratigraphy" section, this chapter) indicate a late Eocene age (35–36 Ma) for this core. The low resolution of these data does not permit a firm correlation of the normal polarity magnetozone to the geomagnetic polarity time scale, and this remanence might represent Chrons C15n, C16n.1n, or C16n.2n.

Cores 152-915A-18R though -22R all record negative inclinations, indicating a reverse polarity remanence. Cores 152-915A-1R to -20R are barren of nannofossils. Cores 152-915A-21R and -22R yielded a nannofossil age of 38 to 41 Ma (middle Eocene), and correlation with Chron C18r is tentatively proposed. It is likely that the reverse polarity remanence recognized throughout Cores 152-915A-1R to -20R records the younger part of the same chron, though we cannot reject the possibility that these are record(s) of younger chrons (i.e., C16r or C17r). If these cores had been deposited sometime after Chron C18r, the dominance of a normal-polarity geomagnetic field during that period (fig. 29 of Cande and Kent, 1992) suggests that some normal-polarity (Chrons C18n and C17n) magnetized sediments would have been deposited. Were this the case at Site 915, we might have expected to recover some of these normally magnetized rocks during the drilling of Hole 915A.

Core 152-915A-24R through the upper part of the volcanic basement also recorded negative inclinations, indicative of a reverse polarity magnetization. Unfortunately, no biostratigraphic data are available from the sediments that immediately overlie the lavas. Instead, the magnetochron correlation has been on the age of the magnetic anomalies in this area, which suggest a Chron C24r age. We anticipate that post-cruise Ar-Ar radiometric dating of these rocks will provide a more firm magnetochron assignment for the volcanic basement. The arguments presented above concerning magnetochron correlations suggest that a hiatus of about 13 m.y. separates the top of the volcanic pile from the base of the sedimentary sequence. Sedimentological observations (see "Lithostratigraphy" section, this chapter) suggest that this hiatus probably marks a period of subaerial exposure. Thus, it is possible that the flows recovered in Hole 915A do not represent the youngest flows that were originally present at this site.

SEDIMENTATION RATES

Five age-control points are available for constructing an age-vs.-depth diagram for Site 915 (Fig. 9), as follows:

1. Core 152-915A-3R (about 13 mbsf) is younger than the Pliocene/Pleistocene boundary (1.8 Ma), according to planktonic foraminiferal data (Fig. 5). This suggests a minimum sedimentation rate of 0.7 cm/k.y. for the interval from the seafloor to 13 mbsf.

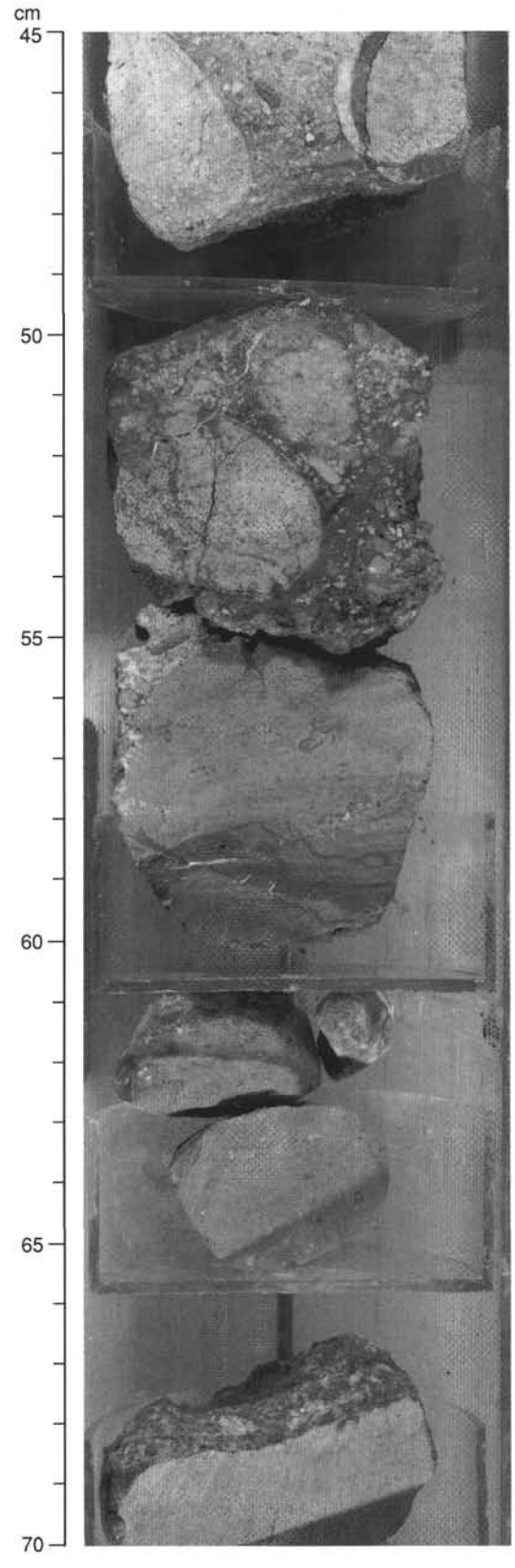

Figure 4. Well-rounded clasts of basalt are interbedded with red sandstone in lithologic Unit III (interval 152-915A-23R-1, 45–70 cm).

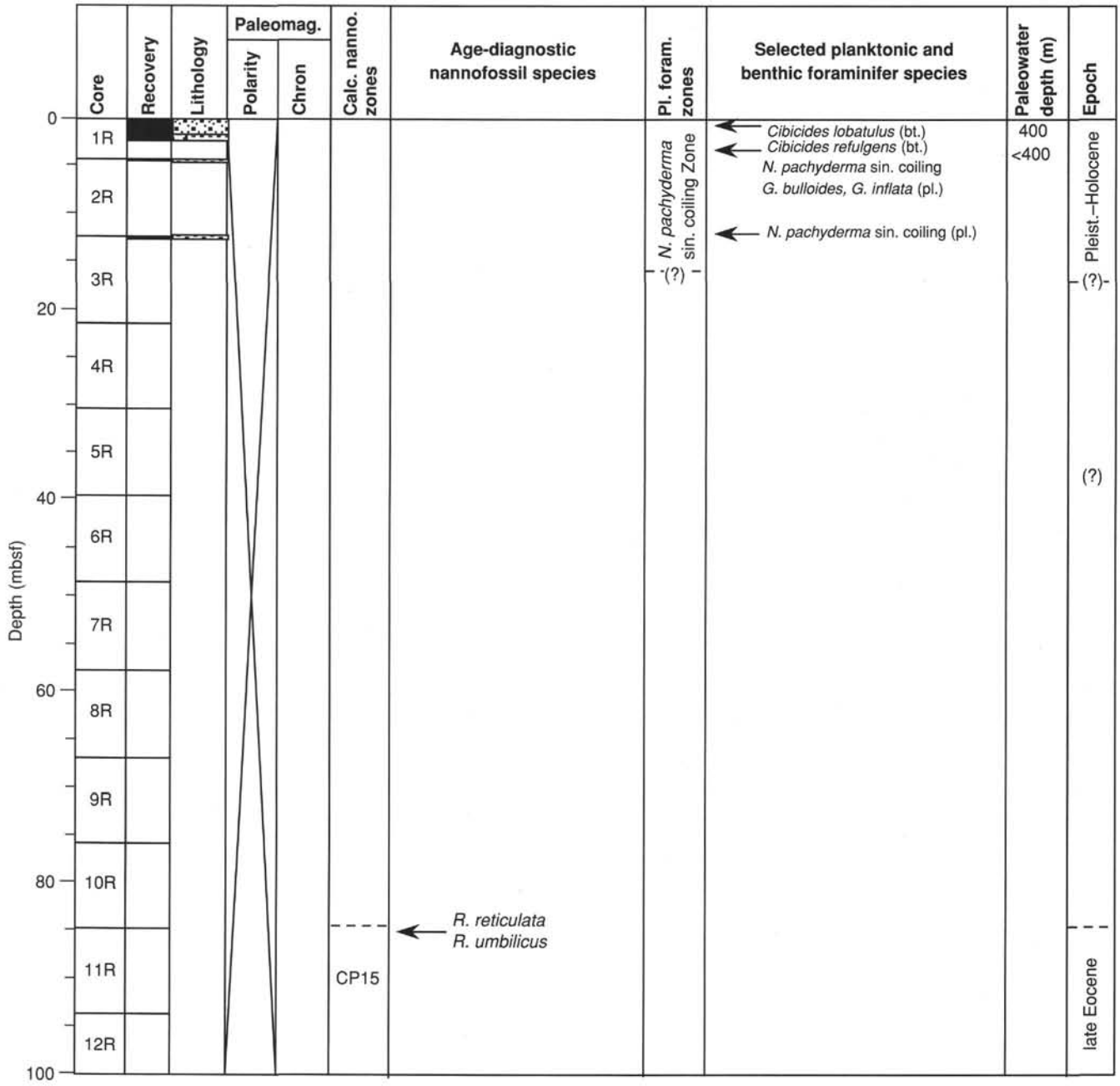

Figure 5. Biostratigraphic summary of Hole 915A. Paleowater depths inferred by benthic foraminiferal species also are shown. bt. = benthic foraminifers, pl. = planktonic foraminifers.

2. Core 152-915A-11R (about 85 mbsf) is older than 35 Ma, according to nannofossil biochronology.

3. Nannofossil biochronology suggests a maximum age of 37 Ma for Core 152-915A-17R (about 140 mbsf). The sedimentation rate between points 2 and 3 (81–140 mbsf) thus is at least 2.95 cm/k.y.

4. The top of Core 152-915A-21R (168 mbsf) is younger than the top of Chron C18r (40.3 Ma), according to the biostratigraphic and magnetostratigraphic interpretations in Figure 5.

5. Section 152-915A-22R-CC (181 mbsf) is younger than Chron C19n (41.4 Ma). The interval between 168 and 181 mbsf thus has a minimum sedimentation rate of 1.2 cm/k.y.

IGNEOUS PETROLOGY

Volcanic rocks were encountered under lithologic Unit III in Section 152-915A-23R-2, 65 cm (189.0 mbsf) and were cored to the bottom of Hole 915A at 209.4 mbsf in Section 152-915A-26R-1. The recovered section consists of two basaltic flow units: an upper unit that is 1 m thick and a lower unit that is at least 9 m thick, of which 3.5 m were recovered. The two units are separated by a poorly recovered sedimentary unit located in Section 152-915A-24R-1, 55–70 cm. Recovery of the sedimentary unit was limited to a few rounded to angular cobbles. The largest of these is a cobble of greenschist facies

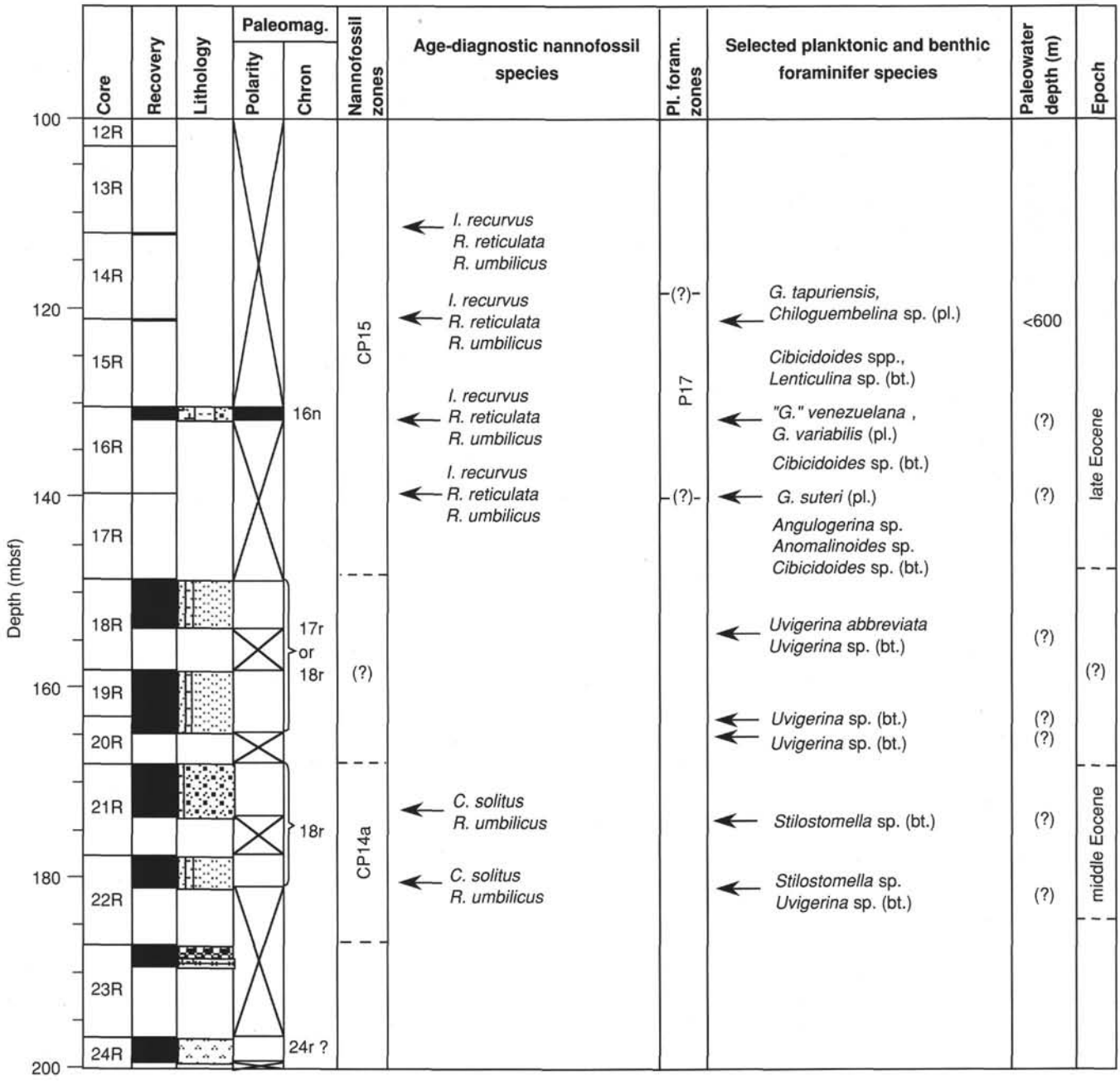

Figure 5 (continued).

metabasalt (Piece 1), while the others are dolerite or vesicular basalt. The upper unit consists of thoroughly oxidized and altered vesicular basalt. None of the primary igneous minerals have been preserved; the rock has been completely weathered to an assemblage dominated by clays.

In contrast, the lower unit is a relatively fresh plagioclase-pyroxene-olivine glomeroporphyritic basalt. The glomerocrysts constitute about 5% of the rock and are composed of plagioclase (An_{68}) with small amounts of augite and olivine. Examination of thin sections revealed magnetite phenocrysts in the coarsest-grained sample (152-915A-24R-2, 51–52 cm [Pc. 2B]). Both phenocryst and groundmass olivine have been completely altered to green clay, but the other mineral phases are fresh. The flow is moderately vesicular (up to 15%) with clay-filled, spherical to irregular vesicles up to 10 mm in diameter. The vesicles are aligned in pipelike trains in Section 152-915A-24R-3. Neither the upper nor lower contacts of the flow are present in the core, so the morphology and original thickness of the flow are unknown.

Chemical analyses of a representative sample of basalt from the lower volcanic unit are given in Table 3. The low Ni and Cr contents suggest that the magma has been moderately evolved, which is in accord with the phenocryst assemblage. The abundances of incompatible elements are low and comparable with abundances in basaltic rocks from Site 917.

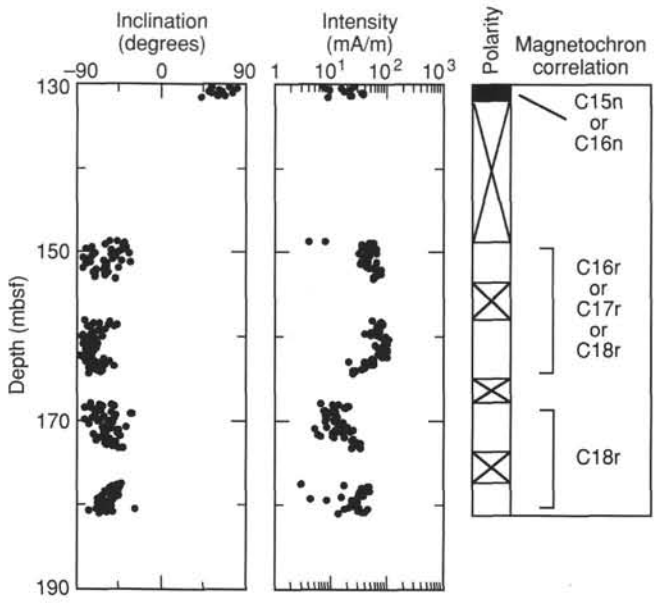

Figure 6. The 30-mT WCC paleomagnetic data for Cores 152915A-16R to -22R. Shown are the inclination and intensity data and the inferred polarity of the core. Biostratigraphic data permit a variety of chron correlations for the polarity data (see text).

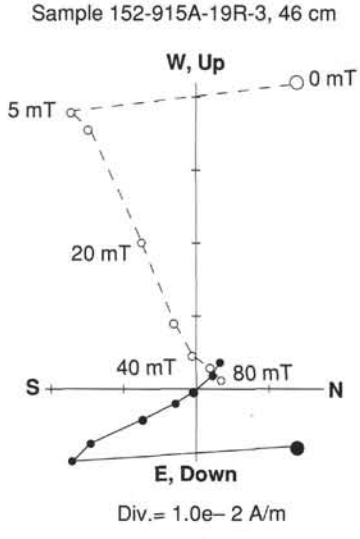

Figure 7. Example of a demagnetization orthogonal projection diagram (Zijderveld, 1967) for a sediment sample (152-915A-19R-3, 46 cm). Solid symbols represent points on the horizontal plane; open symbols, points on the vertical plane. Demagnetization step values are shown adjacent to the vector plotted on the vertical plane. AF demagnetization between 5 and 80 mT reveals a reverse-polarity characteristic magnetization. Note that in this example a high coercivity (>80 mT) magnetic component still resides within the sample.

ORGANIC GEOCHEMISTRY

Volatile Hydrocarbons

As part of the shipboard safety and pollution monitoring program, concentrations of methane (C_1) and ethane (C_2) were monitored in every core in which sediment was recovered, using standard ODP headspace-sampling technique. No significant amounts of gases were detected in the entire sediment column of Site 915.

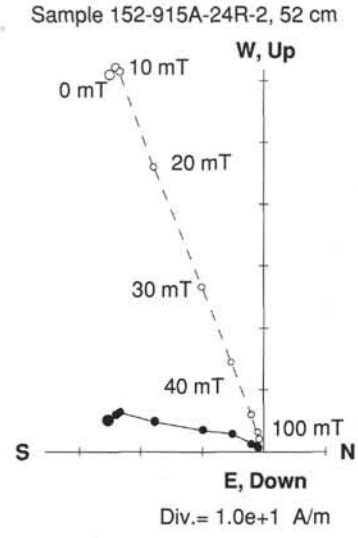

Figure 8. Example of a demagnetization orthogonal projection diagram for a volcanic sample (152-915A-24R-2, 52 cm). See Figure 7 for an explanation of the symbols. Demagnetization to 80 mT reveals a single component with a reverse polarity.

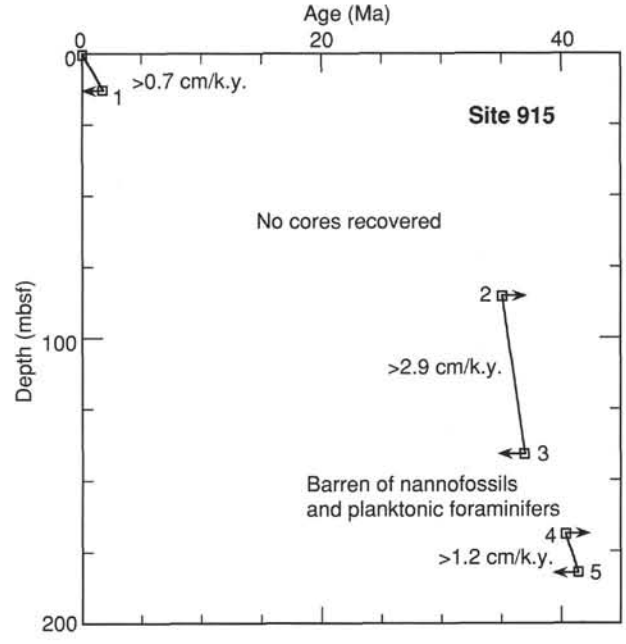

Figure 9. Diagram of age vs. depth for Site 915. Sedimentation rates for different stratigraphic intervals also are shown. See text for explanation of age-control points.

Elemental Analyses

As a result of limited core recovery at Site 915, only 15 sediment samples from Cores 152-915A-18R to -22R were analyzed. Results are presented in Table 4 and Figures 10 and 11. Organic carbon values of the sediments vary between 0.18 and 0.73 wt%. The total nitrogen and total sulfur content ranges from 0.02 to 0.04 wt% and from 0.09 to 1.19 wt%, respectively. Except for Samples 152-915A-21R-3, 12 cm, and -22R-2, 28 cm (20 and 38 wt% $CaCO_3$, respectively), the sediments of Site 915 display very low carbonate contents of between 0 and 0.5 wt%.

Table 3. X-ray fluorescence analyses of basalt (Unit 3).

Major elements (wt%)			Trace elements (ppm)	
	Sample 1	Sample 2		Sample 2
SiO_2	50.15	50.01	V	318
TiO_2	0.93	1.00	Cr	111
Al_2O_3	14.13	14.13	Ni	75
Fe_2O_3	13.30	13.55	Cu	79
MnO	0.18	0.19	Zn	89
MgO	7.79	7.25	Rb	5.8
CaO	11.34	11.76	Sr	66.5
Na_2O	1.79	1.67	Y	27.6
K_2O	0.21	0.15	Zr	50.5
P_2O_5	0.05	0.06	Nb	2.5
			Ba	33
Total	99.87	99.77	Ce	4
LOI	1.03	0.58		

Notes: Sample 1, 152-915A-24R2, 52–56 (Piece 2B) (major elements only). Sample 2, 152-915A-25R1, 31-34 (Piece7). LOI = loss on ignition. Analysts were Don Sims and Mary Ann Cusimano.

The Quaternary diamictons and sandstones described at Site 914 (see "Lithostratigraphy" section, "Site 914" chapter, this volume) contain small amounts of carbonate detritus. Organic matter content is very low as a result of the absence of a vegetation cover within the glacial environment. In the Eocene sandy siltstones and silty sandstones of Site 914 (lithologic Unit II) and Site 915 (lithologic Subunits IIB and IIC), however, calcium carbonate is conspicuously absent (Figs. 10 and 11). Two carbonate-cemented sandstones were sampled at Site 915 at Cores 152-915A-21R (171.2 mbsf) and -22R (179.28 mbsf; Fig. 10). This secondary cementation coincides with glauconite grains (see "Lithostratigraphy" section, this chapter), indicating formation under very low sedimentation rates.

Increased amounts of total sulfur in the sediments of lithologic Subunit IIC (Table 4 corresponds with the common occurrence of finely dispersed pyrite noted in the smear-slide descriptions (see "Lithostratigraphy" section, this chapter).

Composition of Organic Matter

The organic matter in the sediments of Site 915 consists mainly of plant debris, also described in the "Lithostratigraphy" section of the "Site 915" chapter (this volume). A major amount of terrigenous organic matter is confirmed by organic carbon/total nitrogen ratios of up to 20 (Figs. 10 and 11; Table 4). The average TOC-TN ratios of marine planktonic material are between 5 and 8. Higher plants show TOC/TN values between 15 and 200 (Bordovskiy, 1965; Emerson and Hedges, 1988). Note, however, that the amount of inorganic nitrogen in organic carbon-poor sediments (fixed as ammonium ions in the interlayers of clay minerals) may become a major portion of the total nitrogen (Mueller, 1977), causing anomalously low TOC-TN ratios.

INORGANIC GEOCHEMISTRY

Only six interstitial-water samples were obtained at Site 915. Methods are described in the "Inorganic Geochemistry" section of the "Explanatory Notes" chapter (this volume). The results obtained are presented in Table 5. The significance of the results is discussed in the "Inorganic Geochemistry" section of "Site 916" chapter (this volume). This is justified, because Sites 914, 915, and 916, which are in close proximity to each other and to the Greenland coast, form a complementary set of data.

PHYSICAL PROPERTIES

Introduction

Following the difficulties encountered with dropstones and diamicton at Site 914, APC and XCB coring was not attempted at Site

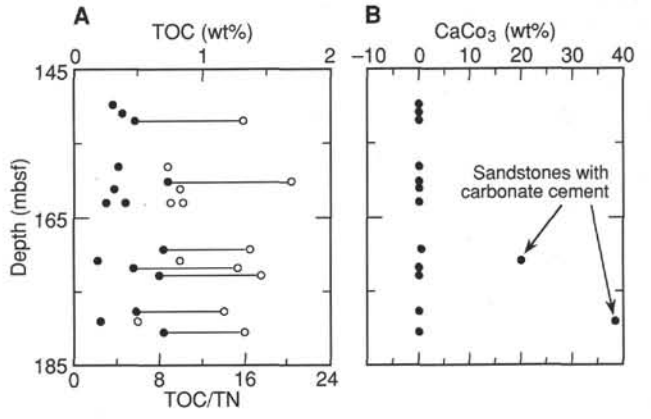

Figure 10. **A.** Results of total organic carbon (TOC = solid circles) and total organic carbon-total nitrogen (TOC/TN = open circles) ratios vs. depth in Hole 915A. Samples having elevated organic carbon content and TOC-TN ratios, indicating significant amounts of terrigenous organic matter, are highlighted with a black line. **B.** Results of calcium carbonate ($CaCO_3$) vs. depth in Hole 915A.

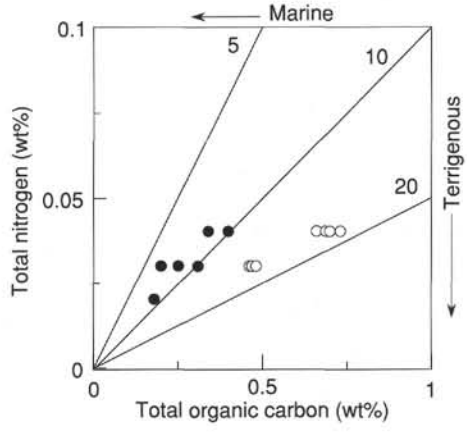

Figure 11. Total organic carbon vs. total nitrogen of Hole 915A. Open circles indicate samples having elevated organic carbon content and high TOC/TN ratios, probably as a result of increased amounts of plant fragments. Samples marked by a solid circle show very low organic carbon contents and should be interpreted with caution.

915. At this site, recovery consists entirely of RCB cores, thus reducing the quality of much of the MST data and preventing continuous measurement of *P*-wave velocity. Owing to the low recovery at Site 915, it was not possible to formulate detailed conclusions regarding downhole changes in mechanical state. However, some good data have been collected at 130 to 133 mbsf and 150 to 185 mbsf. These data may be used to infer gross downhole conditions, particularly with respect to compactional effects on void space, water content, and acoustic velocity. Within the bounds of the data set, correlation with the seismic record is very good.

Multisensor Track (MST)

All stratigraphically continuous cores recovered at Site 915 were processed through the MST. Sections that were made up only of dropstones and/or gravel were not processed. GRAPE wet bulk density, magnetic susceptibility, and natural gamma data were collected during all MST runs. *P*-wave velocities were not measured at Site 915 because recovery consisted of RCB cores only. GRAPE-measured wet bulk density was corrected for drilling disturbance (reduced diam-

Table 4. Summary of organic chemistry analyses at Hole 915A.

Core, section, interval (cm)	Depth (mbsf)	TC (wt%)	IC (wt%)	TOC (wt%)	$CaCO_3$ (wt%)	TN (wt%)	TS (wt%)	TOC/TN ratio
152-915A-								
18R-1, 133–134	149.93	0.30	0.0	0.30	0.00	0.00	0.24	
18R-2, 90–93	151.00	0.37	0.0	0.37	0.00	0.00	0.29	
18R-3, 48–50	152.08	0.47	0.0	0.47	0.00	0.03	0.39	15.77
19R-1, 20–21	158.30	0.34	0.0	0.34	0.00	0.04	0.21	8.72
19R-2, 71–72	160.31	0.73	0.0	0.73	0.00	0.04	0.12	20.28
19R-3, 15–17	161.26	0.31	0.0	0.31	0.00	0.03	0.19	9.84
19R-4, 56–58	163.16	0.25	0.0	0.25	0.00	0.03	0.17	10.16
20R-1, 22–24	163.12	0.40	0.0	0.40	0.00	0.04	0.11	8.98
21R-2, 14–16	169.54	0.76	0.1	0.70	0.50	0.04	1.19	16.37
21R-3, 12–14	171.02	2.58	2.4	0.18	19.99	0.02	0.09	9.83
21R-4, 12–14	171.96	0.46	0.0	0.46	0.00	0.03	0.77	15.23
21R-5, 21–22	173.05	0.66	0.0	0.66	0.00	0.04	1.08	17.39
22R-1, 34–36	177.84	0.48	0.0	0.48	0.00	0.03	0.82	13.97
22R-2, 28–30	179.28	4.78	4.6	0.20	38.15	0.03	0.36	5.91
22R-3, 24–26	180.74	0.69	0.0	0.69	0.00	0.04	1.00	15.95

Note: TC = total carbon; IC = inorganic carbon; TOC = total organic carbon; $CaCO_3$ = calcium carbonate; TN = total nitrogen; TS = total sulfur; TOC/TN = total organic carbon/total nitrogen.

Table 5. Chemical composition of interstitial waters at Site 915.

Core, section, interval (cm)	Depth (mbsf)	pH	Alkalinity (mM)	Salinity (g/kg)	Cl^- (mM)	Ca^{2+} (mM)	Mg^{2+} (mM)	Sr^{2+} (μM)	Li^+ (μM)	Na^+ (mM)	K^+ (mM)	SO_4^{2-} (mM)	NH_4^+ (μM)	H_4SiO_4 (μM)	B (mM)	Mn (μM)
Bottom water		8.10	2.35	34.9	557	10.4	54.0	78	27	480	10.40	29	0	50	0.42	0
152-915A-																
1R-1, 145–150	1.5	8.20	3.57	34.8	557	11.4	47.3	79	22	489	12.00	29.4	105	517	0.51	19.0
15R-CC, 0–5	130.0			32.0	514	27.9	33.0			447	5.80	23.6			0.33	
18R-2, 140–150	150.0	7.65	1.52	30.8	501	29.8	31.3	119	39	420	4.20	21.9	88	135	0.41	17.7
19R-2, 140–150	160.0	7.43	1.10	31.0	504	30.3	30.9	115		423	4.05	22.2	80	119	0.39	18.0
21R-5, 46–56	178.0	8.36	0.95	30.5	496	29.8	28.7	101	31	421	4.10	22.6	114	84	0.29	19.2
22R-2, 145–150	185.0			29.9	486	30.3	27.5	105	32	408	3.90	20.8	111	96	0.28	20.0

eter), as detailed in the "Physical Properties" section of the "Explanatory Notes" chapter (this volume).

As outlined in the "Physical Properties" section of the "Site 914" chapter (this volume), the MST data suite provides an excellent reference for evaluating changes in bulk sediment composition and depositional environments and for correlating stratigraphic events. Cores from Site 915 have been interpreted in terms of mechanical units (see Fig. 15, "Physical Properties" section, "Site 914" chapter, this volume). The uppermost (0.00–0.30 mbsf) sediments recovered in Core 152-915A-1R are characterized by low magnetic susceptibility (400 cgs), natural gamma (700 TC), and high bulk density (2.i0 g/cm^3). These sediments appear to correlate with mechanical Unit M2, recovered in Core 152-914A-1H. At this site, Unit M2 overlies 1.0 m (0.30–1.30 mbsf) of sediment having uniform magnetic susceptibility (400 cgs), natural gamma (700 TC), and somewhat lower bulk density (1.90–2.00 g/cm^3). These lower sediments appear to correlate with mechanical Unit M3, identified in Core 152-914A-1H. A sharp break (1.30 mbsf) in all MST parameters separates Unit M3 from deeper sediments having significantly elevated magnetic susceptibility (950 cgs), natural gamma (1100 TC), and bulk density (2.20 g/cm^3). The elevated MST values and the spiked nature of the data suggest that these sediments correlate with mechanical Unit M4, as defined at Site 914. These spikes were caused by the anomalously high content of radioactive and magnetically susceptible minerals in dropstones.

Core 152-915A-16R was severely biscuited during drilling. Sediments in this core are dominantly indurated, strongly bioturbated nannofossil chalk, interbedded with very dark gray clays and sandy silts. Although the biscuited nature of the core results in noisy MST data, the sediment is characterized by low magnetic susceptibility (≈500 cgs), as expected in carbonate-rich deposits. Higher magnetic susceptibility spikes were caused by interbedded silts and paramagnetic clays. Sediments of this nature were not recovered at Site 914.

Sediments recovered between 147.5 and 181.0 mbsf consist primarily of volcanogenic clastics. These include (1) bioturbated, pyritized clayey siltstones; (2) laminated dusky red clayey silts; (3) calcite-cemented sandstones and silty sandstones; and (4) bioturbated black silts and sands. The interbedded nature of these sediments is clearly evident from the GRAPE wet-bulk-density data, which oscillate between 1.80 and 2.00 g/cm^3 for the brown, sandy silts and between 1.60 and 2.00 g/cm^3 for the reddish, muddy silts. Several high GRAPE bulk-density peaks (up to 2.10 g/cm^3), coincident with magnetic susceptibility troughs, have been interpreted as discrete calcite-cemented bands. Velocities for these cemented sands range as high as 4.5 km/s (see "Velocimetry," this section).

A thin (197.0–189.0 mbsf), complex suite of calcite-cemented, graded volcanic conglomerates, sands, and silts (lithologic Unit III) was recovered in Core 152-915-23R. These sediments are characterized by uniform GRAPE bulk density (≈1.75 g/cm^3), highly variable magnetic susceptibility (from 800 to 1200 cgs), and low natural gamma (≈350 TC). This marked reduction in natural gamma, down from ≈900 TC in the overlying volcaniclastic sandstones, indicates a significant change in either sediment source or post-depositional chemical alteration. The similarity in the signature of these sediments and the underlying weathered and weakly altered basalts suggest that these sediments underwent comparatively little transport. The base of this core contains the strongly weathered top of a lava flow. This weathered material continues in Core 152-915-24R and displays low magnetic susceptibility (≈600 cgs), natural gamma (≈400 TC), and very low GRAPE bulk density (≈1.60 g/cm^3).

The transition to less-altered basalts (at 198.5 mbsf) is marked by sharp increases in GRAPE bulk density (to 2.40 g/cm^3) and magnetic susceptibility (to 1200 cgs). The fragmented nature of Core 152-915A-25R results in a severe degradation in the quality of the MST data.

Index Properties

Wet bulk density, grain density, dry density, water content, porosity, and void ratio (see "Physical Properties" section, "Explanatory Notes" chapter, this volume) have been determined for 27 discrete samples. These data are presented in Table 6 and illustrated in Figure 12.

Wet bulk density of the upper sediments is uniform at 2.10 g/cm^3 for the well-sorted, sandy, interglacial silts, and poorly sorted glacial

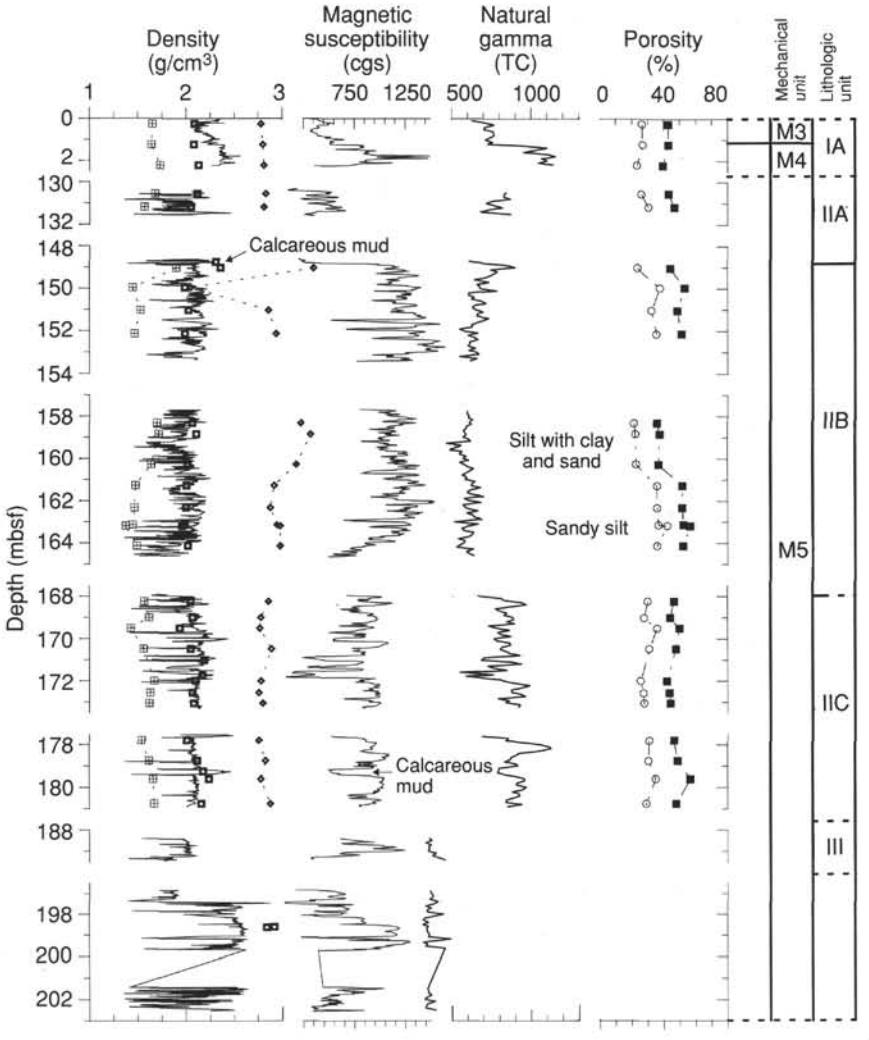

Figure 12. Composite plot of MST and discrete index-property data for sediments recovered at Site 915. MST data comprise GRAPE wet bulk density (corrected for reduced diameter resulting from RCB coring), magnetic susceptibility, and natural gamma. Discrete measurements include wet bulk density (open squares), grain density (open diamonds), dry density (hatched squares), water content (open circles), and porosity (filled squares).

diamictons. For all these sediments, the grain density remains approximately constant at 2.80 g/cm^3. Water content for the interglacial silts is uniform at 27%, whereas in the diamictons, water content is only 23%. As at Site 914, the relative consistency of the grain-density values implies that variations in bulk density (as noted from the GRAPE bulk-density record) must be controlled by fluctuations in water content.

For the deeper volcanogenic sands and silts, variations in water content and porosity appear to depend on the degree of calcite cementation. Hence, variations in grain density result from not only the fluctuation between silt and sand-dominated sediments, but also the degree of cementation. This is especially evident for sediments between 157.0 and 160.0 mbsf, where very high grain densities suggest that significant calcite cementation has filled much of the void space. Note that these sediments have low water content and correspondingly low void ratios. This is supported by the second-order changes in the magnetic susceptibility and natural gamma signals.

Velocimetry

The Hamilton Frame was used to measure compressional (*P*-wave) velocity for 35 cubes cut from the stiff and indurated Tertiary sediments of Cores 152-915A-18R to -22R (130.0–180.0 mbsf) and for two cubes cut from the basalts (198.6–198.8 mbsf). Velocities were measured in three directions: longitudinal (V_z), transverse (V_x), and transverse (V_y) (see "Physical Properties" section, "Explanatory Notes" chapter, this volume). Data are presented in Table 7 and illustrated in Figure 13. No digital sound velocimeter (DSV) data were collected for soft sediments at Site 915, owing to the disturbed nature of the recovered soft sediments in Core 152-915A-1R. The velocities measured for these indurated, weakly cemented, volcaniclastic sediments generally are on the order of 1.7 to 2.0 km/s. Samples from interbedded, calcite-cemented sandstones commonly have acoustic velocities that exceed 3.0 and reach 4.5 km/s, nearly double those of the weakly cemented materials. The transverse velocities (V_x and V_y) in the more laminated samples tend to exceed the longitudinal velocity (V_z). Acoustic velocity in the basalts ranges between 4.6 and 5.0 km/s.

The velocity-depth profile in the Tertiary sediments shows a significant change at 170 mbsf. Above 170.0 mbsf, velocities range between 1.7 and 2.0 km/s and decrease with depth. Below 170 mbsf, velocities are nearly constant at 2.0 km/s. Note that above 170 mbsf, sediments tended to show greater variation in bulk density and frequently were biscuited. Those below 170 mbsf were much more uniform in their bulk density and tended to be recovered in larger coherent pieces. This velocity change between 170.0 and 172.0 mbsf correlates approximately with the boundary between lithologic Units IIB and IIC and with the boundary between the seismic stratigraphic Sequences 4a and 4b, as defined on the seismic profile EG92-24.

A significant impedance contrast exists between the dense, high-velocity, calcite-cemented sandstone and the adjacent medium-density, relatively slow, indurated volcaniclastics. As these layers are of decimeter thickness, it is plausible that some of the reflectors in seismic stratigraphic Sequences 4a and 4b represent the calcite-cemented layers.

Table 6. Index property data for Site 915.

Core, section, interval (cm)	Depth (mbsf)	Water content W_t (%)	Bulk density (g/cm³) MB	Grain density (g/cm³) MC	Dry density (g/cm³) MB	Porosity (%) MC	Void ratio MC
152-915A-							
1R-1, 25–27	0.25	26.66	2.09	2.78	1.65	42.91	0.72
1R-1, 124–126	1.24	26.80	2.08	2.80	1.64	42.86	0.73
1R-2, 72–74	2.22	23.51	2.13	2.81	1.73	39.60	0.65
16R-1, 26–28	130.56	26.31	2.12	2.83	1.68	43.11	0.73
16R-1, 89–91	131.19	30.46	2.05	2.81	1.57	46.76	0.84
18R-1, 42–44	149.02	23.80	2.36	3.33	1.90	44.27	0.77
18R-1, 136–138	149.96	37.66	1.99	2.05	1.45	53.28	0.75
18R-2, 92–94	151.02	32.52	2.03	2.86	1.53	48.60	0.91
18R-3, 52–54	152.12	35.81	1.99	2.94	1.47	51.34	1.03
19R-1, 22–24	158.32	21.74	2.07	3.20	1.70	36.02	0.68
19R-1, 75–77	158.85	22.48	2.11	3.30	1.72	37.83	0.73
19R-2, 68–70	160.28	22.90	2.02	3.15	1.64	36.75	0.70
19R-3, 17–19	161.27	36.01	2.01	2.92	1.48	51.92	1.03
19R-3, 123–125	162.33	36.13	2.00	2.88	1.47	51.75	1.02
19R-4, 59–61	163.19	42.25	1.96	2.98	1.38	56.76	1.23
20R-1, 24–26	163.14	36.90	1.99	2.95	1.45	52.38	1.06
20R-1, 123–125	164.13	35.96	2.02	2.98	1.49	52.16	1.05
21R-1, 35–37	168.25	30.21	2.05	2.86	1.57	46.43	0.84
21R-1, 110–112	169.00	27.87	2.07	2.78	1.62	44.07	0.76
21R-2, 12–14	169.52	35.87	1.94	2.77	1.43	49.93	0.97
21R-2, 108–110	170.48	31.28	2.05	2.89	1.56	47.75	0.88
21R-4, 16–18	172.00	25.83	2.10	2.78	1.67	42.02	0.70
21R-4, 73–75	172.57	27.45	2.07	2.76	1.63	43.56	0.74
21R-5, 22–24	173.06	27.91	2.08	2.80	1.62	44.26	0.76
21R-CC, 23–25	173.63	27.11	2.09	2.87	1.64	43.52	0.76
22R-1, 30–32	177.80	31.11	2.01	2.76	1.54	46.68	0.84
22R-1, 125–127	178.75	30.81	2.12	2.83	1.62	48.85	0.85
22R-2, 61–63	179.61	35.10	2.24	2.78	1.66	56.76	0.95
22R-3, 26–28	180.76	29.28	2.16	2.88	1.67	47.81	0.82

Note: Data were calculated according to Method B (MB) or Method C (MC) as defined in "Physical Properties" section, "Explanatory Notes" chapter (this volume).

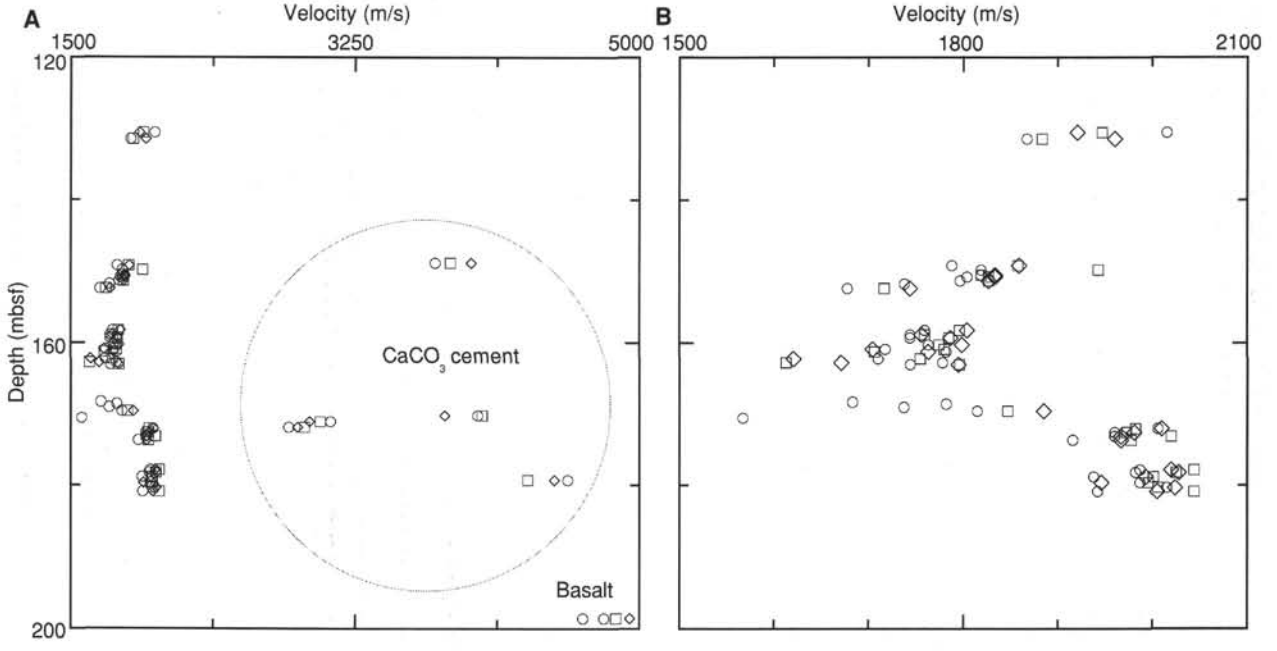

Figure 13. **A.** Discrete longitudinal (V_z) and transverse sonic velocities (V_x and V_y) for sediments recovered in Hole 915A. **B.** Expanded velocity scale to emphasize anisotropic behavior.

Undrained Shear Strength

Soft sediments were recovered only in Core 152-915A-1R. These sediments consisted of sandy, gravelly, low-water-content clays. Peak strengths of 40 and 50 kPa were measured. Results are listed in Table 11, "Physical Properties" section, "Site 914" chapter (this volume) and illustrated in Figure 17, "Physical Properties" section, "Site 914" chapter (this volume).

Resistivity

Resistivity measured for the soft sediments of Core 152-915A-1R ranged from 0.70 to 1.60 kΩm. Resistivity data are listed in Table 12, "Physical Properties" section, "Site 914" chapter (this volume) and illustrated in Figure 18, "Physical Properties" section, "Site 914" chapter (this volume). Insufficient material was available for mini-core testing of the deeper recovered sections.

Thermal Conductivity

Full-space thermal conductivities were measured in Cores 152-915A-1R and 18R through -22R. Values are listed in Table 12, "Physical Properties" section, "Site 914" chapter (this volume) and illustrated in Figure 18, "Physical Properties" section, "Site 914" chapter (this volume). Semi-indurated sediments in the deeper cores were difficult to test, as the sediment often fractured during probe insertion. These sediments were not sufficiently lithified to apply the half-space method. Thermal conductivities for the upper sediments (lithologic Unit I) average 1.40 W/(m·K). Thermal conductivities of the deeper, indurated volcaniclastics (lithologic Unit II) range from 1.30 to 1.60 W/(m·K), higher than typical marine sediments. At 171.0–172.0 mbsf, thermal conductivity decreases to 0.82 W/(m·K). This rapid change correlates with high $CaCO_3$ cement contents and shows a slight increase with depth.

Summary

Core 152-915A-1R comprises mechanical Units M2 through M4, as presented in the "Physical Properties" section of the "Site 914" chapter (this volume). We think that mechanical Unit M1 was not recovered at Site 915. Unit M1 is defined by its very high water content, which decreases rapidly with depth, with a corresponding rapid increase in bulk density. This was not observed in Core 152-915A-1R. Rather, the water content of the surficial sediment is only ≈30%. Mechanical Unit M2 (0.00–0.15 mbsf) consists of a silty sand, which is characterized by comparatively low magnetic susceptibility (400 cgs), natural gamma (700 TC), and bulk density (1.9 g/cm^3).

Ms 152IR-107

Table 7. *P*-wave velocity measurements for Site 915.

Core, section, interval (cm)	Depth (mbsf)	Calculated velocity V_z (m/s)	V_x (m/s)	V_y (m/s)	Comments
152-915A-					
16R-1, 19–21	130.5	2015	1947	1921	
16R-1, 105–107	131.4	1867	1883	1960	
18R-1, 15–17	148.8	3744	3839	3967	
18R-1, 62–64	149.2	1788	1858	1859	
18R-1, 116–118	149.8	1819	1943		
18R-2, 35–37	150.5	1819	1819	1834	
18R-2, 73–75	150.8	1804	1827	1834	
18R-2, 124–126	151.3	1797	1827	1827	
18R-3, 20–22	151.8	1738			
18R-3, 79–81	152.4	1678	1716	1744	
19R-1, 23–25	158.3	1759	1796	1804	
19R-1, 75–77	158.9	1744	1759	1756	
19R-1, 126–128	159.4	1744	1785	1787	
19R-2, 68–70	160.3	1763	1775	1799	
19R-2, 133–135	160.9	1718	1780	1704	Cracked
19R-3, 17–19	161.3	1782	1706	1763	Cracked
19R-3, 122–124	162.3	1710	1755	1621	Poor geometry
19R-4, 24–26	162.8	1778	1613	1671	
20R-1, 23–25	163.1	1744	1796	1795	
21R-1, 64–65	168.5	1782			Half round
21R-1, 110–111	169.0	1737			Half round
21R-1, 35–36	168.3	1683			Half round
21R-2, 12–14	169.5	1815	1847	1885	
21R-2, 65–67	170.1	4004	4032	3802	$CaCO_3$ cemented
21R-2, 110–112	170.5	1567			Very soft
21R-3, 12–14	171.0	3099	3034	2969	Bioturbated
21R-3, 86–88	171.8	2840	2937	2895	Oriented grains
21R-4, 16–18	172.0	2006	1982	2010	
21R-4, 73–75	172.6	1960	1973	1981	
21R-5, 22–24	173.1	1960	2020	1967	
21R-cc, 23–25	173.6	1916	1978	1967	
22R-1, 30–32	177.8	1987	2044	2020	
22R-1, 69–71	178.2	1982	2025	2028	
22R-1, 125–127	178.8	1938	2001	1993	
22R-2, 25–27	179.3	4561	4316	4477	$CaCO_3$ cemented
22R-2, 61–63	179.6	1987	1996	1946	
22R-2, 125–127	180.3	2015	2006	2024	
22R-3, 26–28	180.8	1942	2044	2005	
24R-2, 52–54	198.6	4654	4858	4943	
24R-2, 54–56	198.6	4783			

Note: Longitudinal velocity V_z is perpendicular to core axis, transverse velocity V_x is parallel to bedding strike, transverse velocity V_y is perpendicular to bedding strike (see "Physical Properties" section, "Explanatory Notes" chapter, this volume).

NOTE: For all sites drilled, core-description forms ("barrel sheets") can be found in Section 4, beginning on page 303. Forms containing smear-slide data can be found in Section 5, beginning on page 925. Thin-section data are given in Section 6, beginning on page 947. GRAPE, Index property, MAGSUS and Natural gamma-ray data are presented on CD-ROM (back pocket).